Impacts of phytoplankton availability on bigeye tuna (*Thunnus obesus*) recruitment in the Indian Ocean

Yang Wang[1], Yuying Zhang[2], Jiangfeng Zhu[1*], Xiaojie Dai[1]

1. College of Marine Sciences, Shanghai Ocean University, Shanghai 201306, China;
2. Department of Biological Sciences, Florida International University (Biscayne Bay Campus), North Miami Beach, FL 33181, USA

*Corresponding author, Email: jfzhu@shou.edu.cn

Abstract

Continued and substantial recruitment is one of the keys to sustainable fisheries. In the early life stage, fish larvae have extremely high mortality. Foraging success is one of the most important components of recruitment. In this study, we analyzed the influence of phytoplankton availability on the recruitment success of bigeye tuna in the Indian Ocean. Indian ocean was divided into four regions based on the spatial structure of the bigeye tuna stock assessment. The results showed prey availability has a significant positive influence on recruitment, especially in the eastern and southern Indian Ocean.

Keywords: Bigeye tuna, Indian Ocean, larvae survival, recruitment, stock assessment

1. Introduction

Bigeye tuna (*Thunnus obesus* Lowe, 1983) is one of the most important commercial species in the Indian Ocean, and its commercial value remain increasing over recent decades (Zudaire et al., 2022). Understanding the relationship between the phytoplankton and the recruitment of bigeye tuna could enhance the efficiency of fishery management and also provide useful information for the parameter setting of the stock assessment.

Recruitment is one of the most important processes in fish population dynamics and are responsible for sustainable fishery. After the heavily harvested, the fish populations still exist or even at sustainable levels which rely on substantial compensatory and density-dependent mortality (Camp et al., 2020). The spawning of bigeye tuna has seasonal and year-round characteristics. Spawning occurs in tropical waters when the surface water temperature exceeds ~24 ℃ (Nishikawa and Kenkyūjo, 1985; Schaefer, 2001; Muhling et al., 2017). After the adults spawned, the eggs could hatch into larvae (~3mm long) in a few days, and develop foraging and swimming organs fast, then grow into juveniles in the first month of life (Miyashita et al., 2001; Reglero et al., 2014).

However, throughout the hatching and early life stages, eggs experience exceedingly high levels of mortality(Anderson, 1988; Russo et al., 2022; Shropshire et al., 2022). The biotic and abiotic conditions (e.g. temperature, zooplankton biomass, and eddies) of the water column, particularly the surface layers, can strongly influence the distribution and the abundance of the fish larval stages, thereby affecting the reproductive success of many fish species (Cuttitta et al., 2018; Russo et al., 2022). The feeding success of larvae is hypothesized to be an important source of larval mortality (Anderson, 1988; Llopiz and Hobday, 2015). In particular, species like bigeye tuna mainly spawn in tropical regions where prey availability may be more determinant than the temperature for larval survival (Reglero et al., 2014; Shropshire et al., 2022). Upon yolk sack absorption, tuna larvae depend entirely on zooplankton to meet their metabolic requirements (Llopiz and Hobday, 2015; Shropshire et al., 2022). Because of this shift from endogenous nutrition to exogenous, the larvae are most sensitive at this time to environmental factors, particularly food supply. A higher specific mortality rate often occurs immediately following the period of strictly endogenous yolk feeding, and during the period of first exogenous feeding. This period was hypothesized as “critical period” (Hjort, 1914).

However, over the decades of research, the hypotheses of “critical period” driving recruitment success remain equivocal and controversial (Sifa and Mathias, 1987; Robert et al., 2013). The research on the larval foraging success of bigeye tuna is still limited. And the most of information about the tunas' recruitment and reproduction is available for the Pacific Ocean (Langley et al., 2009; Zhu et al., 2010; Sun et al., 2013; Muhling et al., 2018; Woodworth-Jefcoats and Wren, 2020). Therefore, our goal for this study is to test whether the "critical period" hypothesis is tenable for bigeye tuna in the Indian Ocean. We used median phytoplankton size (M_{D50}) as the proxy for the food quality of the larval. Greater value of M_{D50} would mean that there are more large phytoplankton and in turn more prey available for the zooplankton upon which larval bigeye tuna feed (Polovina and Woodworth, 2012; Llopiz and Hobday, 2015). We tested the relationship between M_{D50} and the environment-related parameters of the Beverton-Holt stock-recruitment function (B-H function) (Beverton and Holt, 1957). And we also compared the relationships in different regions of the Indian Ocean based on the spatial stratification of the latest stock assessment model of bigeye tuna (Fu, 2019). We hope the results could help to improve the parameter setting in the bigeye tuna stock assessment.

2. Materials and methods

2.1 Spatial Stratification

The research area of this study covered the whole Indian Ocean and was divided into four regions based on the spatial structure used in the current assessment: South-western equatorial region (R1S), North-western equatorial region (R1N), eastern equatorial region (R2) and southern region (R3) (Fu, 2019). The western equatorial region (R1) was partitioned at the equator to account for differences in the distribution of tags.

2.2 Environmental data

M_{D50} (cell size) in equivalent spherical diameter (ESD) in μm is transformed from cell mass (M_{B50}) which is calculated as Equation 1:

$$\log_{10}(M_{B50}) = 0.929\left(\log_{10}(chla)\right) - 0.043(SST) + 1.340 \quad (1)$$

Where chla is chlorophyll-a in mg/m3, and SST is sea surface temperature in °C. Then convert M_{B50} to M_{D50} as Equation 2:

$$M_{D50} = 2.138(M_{B50})^{0.355} \quad (2)$$

As we can't find continuous chl-a data before 2000, chl-a data was selected from 2000 to 2018 conducted by NASA mission Moderate-resolution Imaging Spectroradiometer (MODIS) Terra Chlorophyll Data (Terra/MODIS) (NASA Goddard Space Flight Center, 2018). SST data come from NOAA Extended Reconstructed SST v5 (Huang et al., 2017).

2.3 Beverton-Holt stock-recruitment function

The B-H Stock-recruitment functions express the production of new recruits to a fish population and the dependence of that production on the spawning component of the population (Miller and Brooks, 2021). The basic function as Equation 3:

$$\frac{R}{S} = \frac{1}{\alpha S + \beta} \quad (3)$$

where R is the number of recruits, S is the spawning biomass. The parameters α and β are related two types of mortality. In which, β refers to the mortality caused by external (or density-independent) factors, such as temperature, wind, currents, and prey availability. Whereas, α is mainly related to density-independent mortality rates (Beverton and Holt, 1957; Miller and Brooks, 2021). Therefore, we turn to study the relationship between M_{D50} and β. If there have any significant linear regression, the relationship between M_{D50} and recruitment could be described by the B-H function.

Mace and Doonan (Mace et al., 1988) then introduced the alternative parameterization for the B-H function in terms of steepness Δ, equilibrium unexploited recruitment R_0 or spawning biomass S_0, and the unexploited spawning biomass per recruit $S_0/R_0 = \varphi_0$. Francis (Francis, 1992) introduced h for steepness after, which is more frequently used. We extracted h, R_0, and S_0 data from the bigeye tuna stock assessment model (Fu, 2019), which used the stock synthesis Model Version 3.24z (SS3). The B-H function was defined in the SS3 model as:

$$\frac{R_y}{S_y} = \frac{1}{\frac{5h-1}{4hR_0} \cdot S_y + \frac{(1-h)S_0}{4hR_0}} \tag{4}$$

Where S_y and R_y is the spawning biomass and recruitment during year y. Then combined with the basic function, α can be calculated as:

$$\alpha = \frac{5h-1}{4hR_0} \tag{5}$$

Therefore, β would be:

$$\beta = \frac{S_y}{R_y} - \alpha S_y \tag{6}$$

Bigeye tuna has been routinely assessed by the Indian Ocean Tuna Commission (IOTC). As we mentioned before, we extracted the h, R_0, S_y, and R_y data from the 2018 stock assessment SS model conducted by the IOTC (Fu, 2019). In the model, the annual data were compiled into quarters (Jan−Mar, Apr−Jun, Jul−Sep, Oct−Dec), and a quarterly time step is treated as a model year in the SS3 model. And also, SS3 followed the spatial structure. Therefore, we can gain the values of β for each region by quarter. Based on the spatial and temporal stratification, we calculated the mean values of MD50 correspondingly.

2.4 Z Score Transformation

As the data sets have dissimilar metrics, we standardized them by Z-Score transformation which converts separate distribution into standardized distribution. The z-score formula is:

$$Z = \frac{X - \overline{X}}{s} \tag{7}$$

Where X is the original data value, $\overline{X}$ and s are the mean and standard deviation, respectively. The transformed variable Z will have a mean of 0 and a variance of 1.

3. Results

To display directly, we plotted the distributions of reversed β (refer to recruitment) and M_{D50} for each region (Figure2). As β is in the denominator in the B-H function, the positive relationship between reversed β and M_{D50} means higher M_{D50} will bring higher recruitment. In Figure 2, the M_{D50} showed positively related to the reversed parameter β as we hypothesized. However, for each region, there have some outliers that showed the opposite correlation. For these outliers, although M_{D50} are low, the reversed β are still at the high level. We grouped these points by season, the plots indicated that mainly outliers come from the same season. For the R1N, R2, and R3, outliers mostly in season 2 (Apr−Jun). For the R1S, outliers primarily come from season 3 (Jul−Sep). These “anomalous” seasons offset the correlations of other seasons to some extent. Therefore, we tested two datasets for each area. One is the original data that covered all the time series, another dataset removed the “anomalous” season data. Figure 3 showed the time series of reversed β and M_{D50}. For all regions, the time series of reversed β and M_{D50} have significant similar seasonal trends, especially for the right half of the Figure3 which datasets exclude the “anomalous” season.

As the variables follow the nominal distribution, we used linear regression to analyze the relationships. The models based on the all-seasons data and removed “anomalous” season were defined as Model 1 and Model 2, respectively. The results of linear regression were shown in Table 1 and the values of the Pearson correlation coefficient were shown in Table 2. Based on the Model 1, M_{D50} showed significant negative relationships with β in R1S (p = 0.003, r = -0.333), R2 (p < 0.001, r = -0.371) and R3 (p < 0.001, r = -0.546). No correlation was found in R1N (p = 0.152, r = -0.166). After removing the “anomalous” season, the correlations improved notably in Model 2. β and M_{D50} have significant correlations (p < 0.001) in all regions. Correlation coefficients are -0.544 in R1N, -0.561 in R1S, -0.665 in R2, and -0.677 in R3. The residual diagnostics of the linear regression models were shown as Q-Q plots in Figure 4.

4. Discussion

In this study, we didn't consider the time-lag effects. In the stock assessment, model, new recruitment was defined as occurring in every season (Fu, 2019). As we aimed to verify the food availability in the early life stage, the time of β and M_{D50} should be matched.

Our results provide support to the hypotheses of "critical period". For all regions, reversed β and M_{D50} fit significant positive relationships. With the same scale of degree of freedom, we found that the highest value of correlation coefficient is in the R3 and the second highest value is in the R2. The eastern Indian Ocean (R2 in our study) is believed as the main spawning area of bigeye tuna (Reglero et al., 2014; Muhling et al., 2017). Due to the high density of larvae, food availability becomes more important than R1S and R1N. In the stock assessment model, it's assumed that the recruitment also occurred in R3. R3 is a temperate area which is not an optimal environment for larvae survival. Thus, we speculate that the survival of larvae is more dependent on the food than the equatorial areas.

The results also showed strong seasonal characteristics. Seasons 1 and 4 have lower recruitment and correspond to lower M_{D50} values in all regions. Seasons 2 and 3 have higher recruitment. However, M_{D50} are low in season 2 in R1N, R2, and R3. We suppose that season 2 is the spawning season for bigeye tuna. Even though the food is limited, enormous eggs could also bring a high recruitment level. However, we still can't explain why the spawning season that we supposed is different in R1S. What's more, very limited studies showed that the spawning season of bigeye tuna is from January to April in the western Indian Ocean and December to January and June in the eastern Indian Ocean, which is not consistent with our results (Nootmorn, 2004; Zudaire et al., 2022). As the model time step is artificially divided, we think that the spawning season may be more flexible in real situations. More studies are still needed to explain these results.

5. Reference

Anderson, J.T. (1988). A Review of Size Dependant Survival During Pre-recruit Stages of Fishes in Relation to Recruitment. *Journal of Northwest Atlantic Fishery Science* 8**,** 55-66. doi: 10.2960/j.v8.a6.

Beverton, R.J.H., and Holt, S.J. (1957). *On the dynamics of exploited fish populations.* Springer Dordrecht.

Camp, E., Collins, A.B., Ahrens, R.N., and Lorenzen, K. (2020). Fish Population Recruitment: What recruitment means and why it matters. *EDIS* 2020(2)**,** 6. doi: https://doi.org/10.32473/edis-FA241-2022.

Cuttitta, A., Torri, M., Zarrad, R., Zgozi, S., Jarboui, O., Quinci, E.M., et al. (2018). Linking surface hydrodynamics to planktonic ecosystem: the case study of the ichthyoplanktonic assemblages in the Central Mediterranean Sea. *Hydrobiologia* 821(1)**,** 191-214. doi: 10.1007/s10750-017-3483-x.

Francis, R. (1992). Use of Risk Analysis to Assess Fishery Management Strategies: A Case Study using Orange Roughy (Hoplostethus atlanticus) on the Chatham Rise, New Zealand. *Canadian Journal of Fisheries and Aquatic Sciences* 49**,** 922-930.

Fu, D. (2019). Preliminary Indian Ocean Bigeye Tuna Stock Assessment 1950-2018 (Stock Synthesis). IOTC–2019–WPTT21–61.

Hjort, J. (Year). "Fluctuations in the great fisheries of northern Europe viewed in the light of biological research": Rapp. Conserv. Explor. Mer).

Huang, B., Thorne, P.W., Banzon, V.F., Boyer, T., Chepurin, G., Lawrimore, J.H., et al. (2017). "NOAA Extended Reconstructed Sea Surface Temperature (ERSST), Version 5. [indicate subset used].". NOAA National Centers for Environmental Information).

Langley, A., Briand, K., Kirby, D.S., and Murtugudde, R. (2009). Influence of oceanographic variability on recruitment of yellowfin tuna (Thunnus albacares) in the western and central Pacific Ocean. *Canadian Journal of Fisheries and Aquatic Sciences* 66(9)**,** 1462-1477. doi: 10.1139/F09-096.

Llopiz, J.K., and Hobday, A.J. (2015). A global comparative analysis of the feeding dynamics and environmental conditions of larval tunas, mackerels, and billfishes. *Deep Sea Research Part II: Topical Studies in Oceanography* 113**,** 113-124. doi: https://doi.org/10.1016/j.dsr2.2014.05.014.

Mace, P.M., Doonan, I.J., and Fisheries, M. (1988). *A Generalised Bioeconomic Simulation Model for Fish Population Dynamics.* MAFFish, N.Z. Ministry of Agriculture and Fisheries.

Miller, T.J., and Brooks, E.N. (2021). Steepness is a slippery slope. *Fish and Fisheries* 22(3)**,** 634-645. doi: https://doi.org/10.1111/faf.12534.

Miyashita, S., Sawada, Y., Okada, T., Murata, O., and Kumai, H. (Year). "Morphological development and growth of laboratory-reared larval and juvenile Thunnus thynnus (Pisces: Scombridae)": Fish Bull), 601-616.

Muhling, B.A., Lamkin, J.T., Alemany, F., García, A., Farley, J., Ingram, G.W., et al. (2017). Reproduction and larval biology in tunas, and the importance of restricted area spawning grounds. *Reviews in Fish Biology and Fisheries* 27(4)**,** 697-732. doi: 10.1007/s11160-017-9471-4.

Muhling, B.A., Tommasi, D., Ohshimo, S., Alexander, M.A., and DiNardo, G. (2018). Regional-scale surface temperature variability allows prediction of Pacific bluefin tuna recruitment. *ICES Journal of Marine Science* 75(4)**,** 1341-1352. doi: 10.1093/icesjms/fsy017.

NASA Goddard Space Flight Center, O.E.L., Ocean Biology Processing Group. (2018). "MODIS-TERRA Level 3

Mapped Chlorophyll Data Version R2018.0 [Data set]". NASA Ocean Biology DAAC).

Nishikawa, Y., and Kenkyūjo, S.E.S. (1985). *Average distribution of larvae of oceanic species of Scombroid fishes, 1956-1981.* Far Seas Fisheries Research Laboratory.

Nootmorn, P. (2004). Reproductive Biology of Bigeye tuna in the eastern Indian ocean. *WPTTO 04-05,IOTC Proceedings*.

Polovina, J.J., and Woodworth, P.A. (2012). Declines in phytoplankton cell size in the subtropical oceans estimated from satellite remotely-sensed temperature and chlorophyll, 1998–2007. *Deep Sea Research Part II: Topical Studies in Oceanography* 77-80**,** 82-88. doi: https://doi.org/10.1016/j.dsr2.2012.04.006.

Reglero, P., Tittensor, D.P., Álvarez-Berastegui, D., Aparicio-González, A., and Worm, B. (2014). Worldwide distributions of tuna larvae: revisiting hypotheses on environmental requirements for spawning habitats. *Marine Ecology Progress Series* 501**,** 207-224.

Robert, D., Murphy, H.M., Jenkins, G.P., and Fortier, L. (2013). Poor taxonomical knowledge of larval fish prey preference is impeding our ability to assess the existence of a "critical period" driving year-class strength. *ICES Journal of Marine Science* 71(8)**,** 2042-2052. doi: 10.1093/icesjms/fst198.

Russo, S., Torri, M., Patti, B., Musco, M., Masullo, T., Di Natale, M.V., et al. (2022). Environmental Conditions along Tuna Larval Dispersion: Insights on the Spawning Habitat and Impact on Their Development Stages. *Water* 14(10). doi: 10.3390/w14101568.

Schaefer, K.M. (2001). "Reproductive biology of tunas," in *Fish Physiology*. Academic Press), 225-270.

Shropshire, T.A., Morey, S.L., Chassignet, E.P., Karnauskas, M., Coles, V.J., Malca, E., et al. (2022). Trade-offs between risks of predation and starvation in larvae make the shelf break an optimal spawning location for Atlantic bluefin tuna. *Journal of Plankton Research* 44(5)**,** 782-798. doi: 10.1093/plankt/fbab041.

Sifa, L., and Mathias, J.A. (1987). The critical period of high mortality of larvae fish —A discussion based on current research. *Chinese Journal of Oceanology and Limnology* 5(1)**,** 80-96. doi: 10.1007/BF02848526.

Sun, C.L., Yeh, S.Z., Chang, Y.J., Chang, H.Y., and Chu, S.L. (2013). Reproductive biology of female bigeye tuna Thunnus obesus in the western Pacific Ocean. *Journal of Fish Biology* 83(2)**,** 250-271. doi: https://doi.org/10.1111/jfb.12161.

Woodworth-Jefcoats, P.A., and Wren, J.L.K. (2020). Toward an environmental predictor of tuna recruitment. *Fisheries Oceanography* 29(5)**,** 436-441. doi: https://doi.org/10.1111/fog.12487.

Zhu, G., Dai, X., Xu, L., and Zhou, Y. (2010). Reproductive biology of Bigeye Tuna, Thunnus obesus, (Scombridae) in the eastern and central tropical Pacific Ocean. *Environmental Biology of Fishes* 88(3)**,** 253-260. doi: 10.1007/s10641-010-9636-7.

Zudaire, I., Artetxe-Arrate, I., Farley, J., Murua, H., Kukul, D., Vidot, A., et al. (2022). Preliminary estimates of sex ratio, spawning season, batch fecundity and length at maturity for Indian Ocean bigeye tuna IOTC-2022-WPTT24(DP)-18.

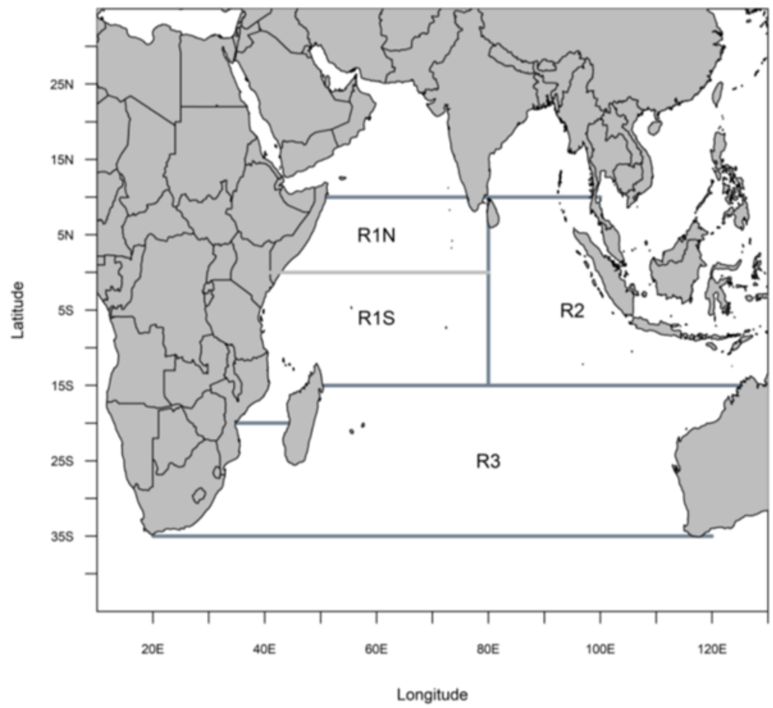

Figure 1: Spatial structure of the stock assessment of the bigeye tuna in the Indian Ocean.

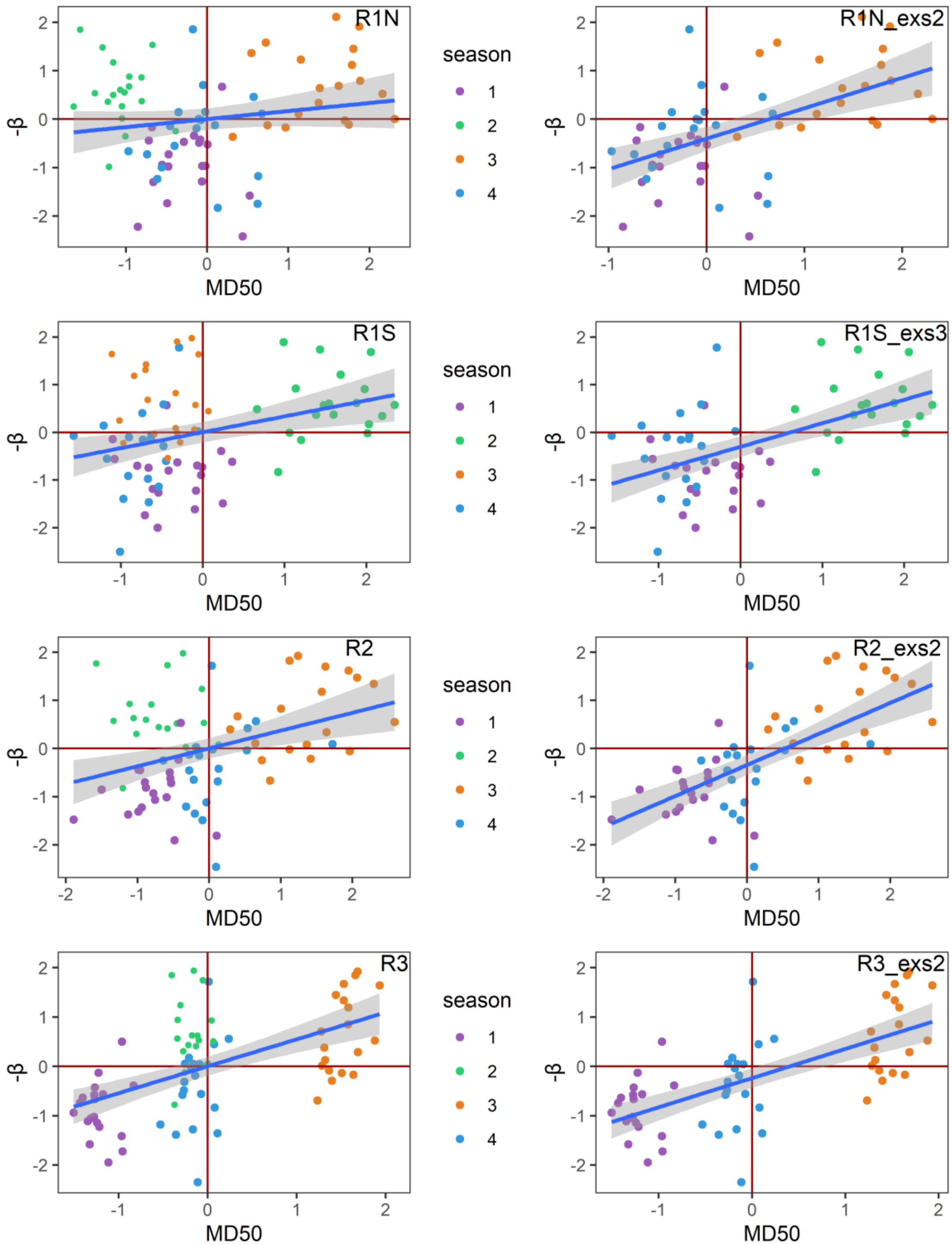

Figure 2. Scatter plots of M_{D50} and reversed β with fitted linear regression lines in four regions. R1N_exs2: exclude season 2 data in R1N. R1S_exs3: exclude season 3 data in R1S. R2_exs2: exclude season 2 data in R2. R3_exs2: exclude season 3 data in R3.

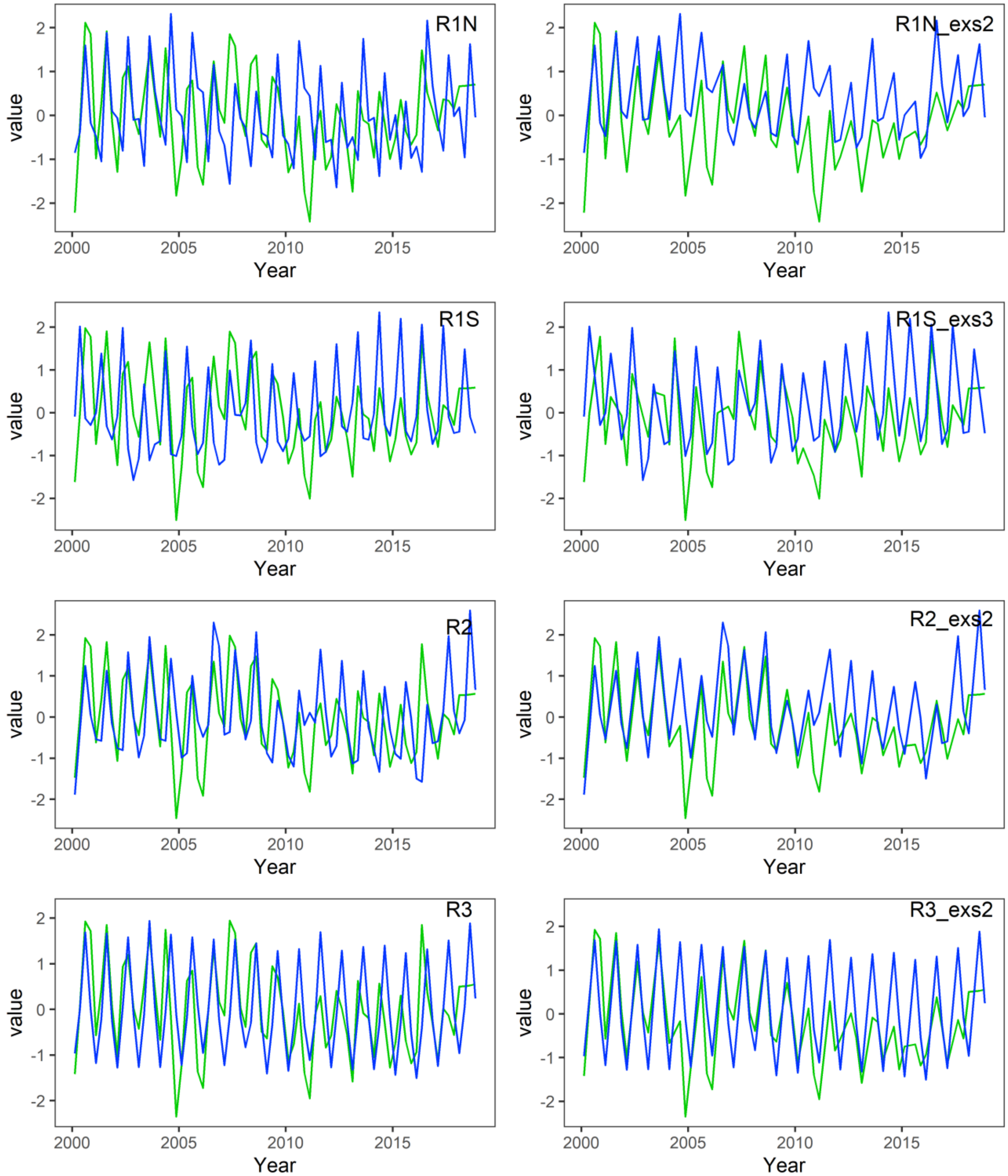

Figure 3. Time series of reversed β (green) and M_{D50} (blue) from 2000 to 2018. R1N_exs2: exclude season 2 data in R1N. R1S_exs3: exclude season 3 data in R1S. R2_exs2: exclude season 2 data in R2. R3_exs2: exclude season 3 data in R3.

Table 1 Summary of regression analysis on β and M_{D50} in four regions. Data in Model 1covered all-seasons data and in Model 2 removed "anomalous" season. SE: stand error; DF: degree of freedom.

	Model1					Model 2				
	Regression equation	SE	DF	p	Adjusted-r^2	Regression equation	SE	DF	p	Adjusted-r^2
R1N	$\beta = -0.17M_{D50}$	0.11	74	0.152	0.014	$\beta = -0.63M_{D50} + 0.4$	0.13	55	< 0.001	0.28
R1S	$\beta = -0.33M_{D50} - 0.9$	0.11	74	0.003	0.1	$\beta = -0.49M_{D50} + 0.3$	0.1	55	< 0.001	0.31
R2	$\beta = -0.37M_{D50} + 0.16$	0.11	74	< 0.001	0.13	$\beta = -0.64M_{D50} + 0.35$	0.09	55	< 0.001	0.43
R3	$\beta = -0.55M_{D50} + 0.14$	0.09	74	< 0.001	0.29	$\beta = -0.59M_{D50} + 0.24$	0.08	55	< 0.001	0.45

Table 2. Correlation coefficient between β and M_{D50} in four regions. Dataset1 covered all-seasons data and Dataset 2 removed "anomalous" season.

	Dataset1 (r)	Dataset 2 (r)
R1N	-0.166	-0.544
R1S	-0.333	-0.561
R2	-0.371	-0.665
R3	-0.546	-0.677

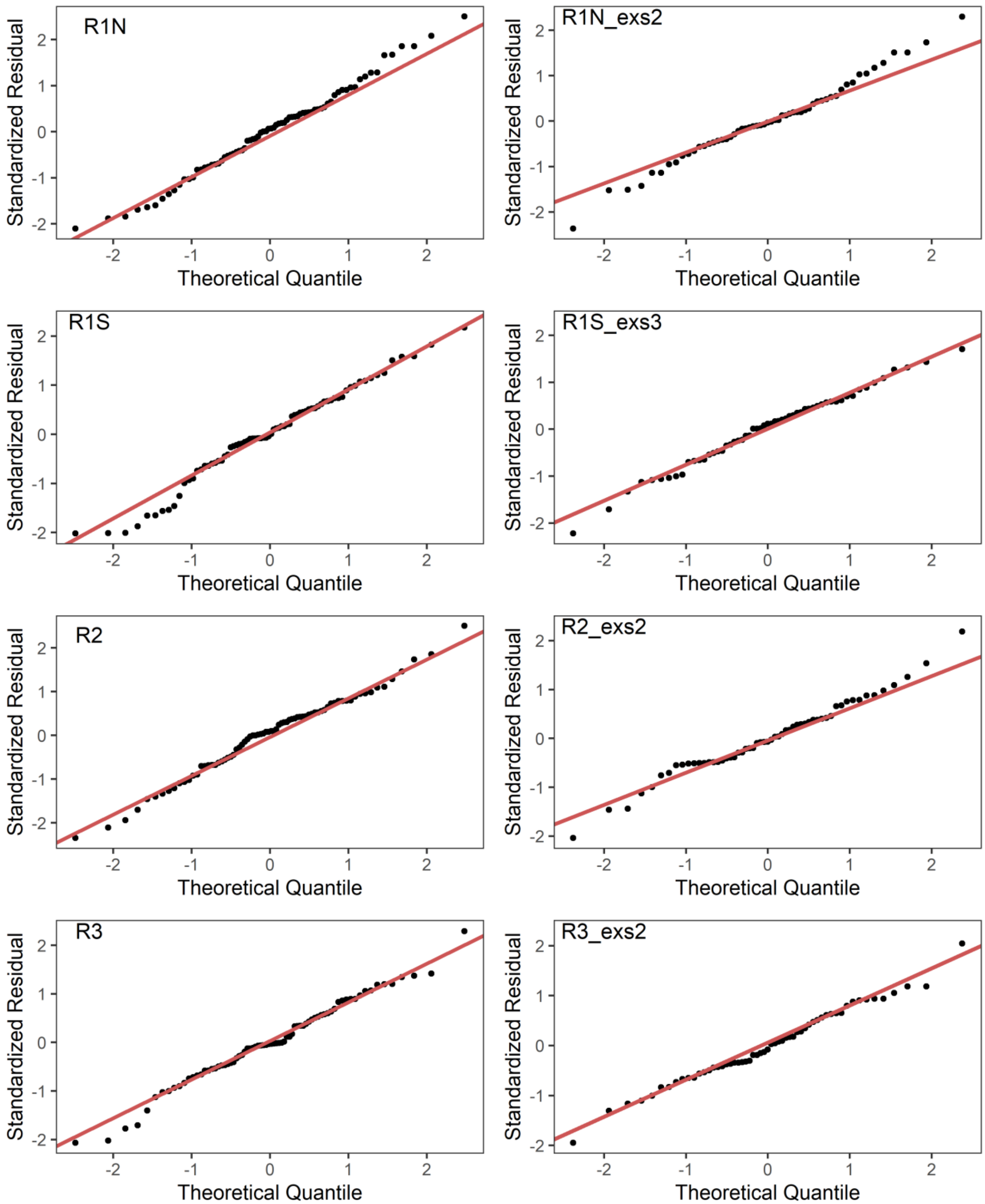

Figure 4. Residual diagnostics of linear regression models as Q-Q plots for four regions. R1N_exs2: exclude season 2 data in R1N. R1S_exs3: exclude season 3 data in R1S. R2_exs2: exclude season 2 data in R2. R3_exs2: exclude season 3 data in R3.